ment. It is clear that the atmosphere in the range up to 600 km is a very complex system that will have to be examined over latitude and season to be understood.

References and Notes

1. L. W. Esposito *et al.*, *Science* **307**, 1251 (2005).
2. Materials and methods are available as supporting material on *Science* Online.
3. G. R. Smith *et al.*, *J. Geophys. Res.* **87**, 1351 (1982).
4. R. J. Vervack Jr., B. R. Sandel, D. F. Strobel, *Icarus* **170**, 91 (2004).
5. F. M. Flasar, *Planet. Space Sci.* **46**, 1109 (1998).
6. F. M. Flasar, *Planet. Space Sci.* **46**, 1125 (1998).
7. C. C. Porco *et al.*, *Nature* **434**, 159 (2005).
8. G. H. Mount, H. W. Moos, *Astrophys. J.* **224**, L35 (1978).
9. G. H. Mount, E. S. Warden, H. W. Moos, *Astrophys. J.* **214**, L47 (1977).
10. H. Sun, G. L. Weissler, *J. Chem. Phys.* **23**, 1160 (1955).
11. H. Okabe, *J. Chem. Phys.* **75**, 2772 (1981).
12. C. Y. R. Wu, F. Z. Chen, D. L. Judge, *J. Geophys. Res.* **106**, 7629 (2001).
13. F. Z. Chen, C. Y. R. Wu, *J. Quant. Spectrosc. Radiat. Transf.* **85**, 195 (2004).
14. C. Y. R. Wu, F. Z. Chen, D. L. Judge, *J. Geophys. Res. Planets* **109** (E7), E07S15, doi:10.1029/2003JE002180 (2004).
15. G. Cooper, G. R. Burton, C. E. Brion, *J. Electron Spectrosc. Relat. Phenom.* **73**, 139 (1995).
16. J. W. Au, G. Cooper, G. R. Burton, T. N. Olney, C. E. Brion, *Chem. Phys.* **173**, 209 (1993).
17. J. A. Nuth, S. Glicker, *J. Quant. Spectrosc. Radiat. Transfer* **28**, 223 (1982).
18. T. Nagata, T. Kondow, Y. Ozaki, K. Kuchitsu, *Chem. Phys.* **57**, 45 (1981).
19. J. A. R. Samson, G. N. Haddad, *J. Opt. Soc. Am.* **64**, 47 (1974).
20. J. A. R. Samson, G. N. Haddad, T. Masuoka, P. N. Pareek, *J. Chem. Phys.* **90**, 6925 (1989).
21. R. V. Yelle, personal communication.
22. D. F. Strobel, M. E. Summers, X. Zhu, *Icarus* **100**, 512 (1992).
23. J. H. Waite Jr. *et al.*, *Science* **308**, 982 (2005).
24. E. H. Wilson, S. K. Atreya, *J. Geophys. Res.* **109**, E06002; doi:10.1029/2003JE002181 (2004).
25. Y. L. Yung, M. Allen, J. P. Pinto, *Astrophys. J.* (suppl. **55**), 465 (1984).
26. A. J. Friedson, Y. L. Yung, *J. Geophys. Res.* **89**, 85 (1984).
27. G. F. Lindal *et al.*, *Icarus* **53**, 348 (1983).
28. R. V. Yelle, D. F. Strobel, E. Lellouch, D. Gautier, Eur. Space Agency Spec. Publ., *ESASP* **1177**, 243 (1997).
29. D. F. Strobel, personal communication.
30. I. C. F. Muller, R. V. Yelle, *Geophys. Res. Lett.* **29**, 2139 (2002).
31. B. Sicardy *et al.*, *AAS/DPS* **36.2206S** (2004).
32. E. Lellouch, D. M. Hunten, G. Kockarts, A. Coustenis, *Icarus* **83**, 308 (1990).
33. The authors thank H. Waite and R. Yelle of the INMS team, D. Strobel for useful comments and for providing data and calculations, E. Wilson for useful discussion and model densities, and L. Bloom for work on the manuscript. This work is one part of the Cassini UVIS investigation supported by the NASA/ Jet Propulsion Laboratory Cassini mission.

Supporting Online Material

www.sciencemag.org/cgi/content/full/308/5724/978/DC1
Materials and Methods
Figs. S1 and S2

3 March 2005; accepted 14 April 2005
10.1126/science.1111790

REPORT

Ion Neutral Mass Spectrometer Results from the First Flyby of Titan

J. Hunter Waite Jr.,[1] Hasso Niemann,[2] Roger V. Yelle,[3] Wayne T. Kasprzak,[2] Thomas E. Cravens,[4] Janet G. Luhmann,[5] Ralph L. McNutt,[6] Wing-Huen Ip,[7] David Gell,[1] Virginie De La Haye,[1] Ingo Müller-Wordag,[8] Brian Magee,[1] Nathan Borggren,[3] Steve Ledvina,[5] Greg Fletcher,[1] Erin Walter,[1] Ryan Miller,[1] Stefan Scherer,[1] Rob Thorpe,[9] Jing Xu,[1] Bruce Block,[1] Ken Arnett[1]

The Cassini Ion Neutral Mass Spectrometer (INMS) has obtained the first in situ composition measurements of the neutral densities of molecular nitrogen, methane, molecular hydrogen, argon, and a host of stable carbon-nitrile compounds in Titan's upper atmosphere. INMS in situ mass spectrometry has also provided evidence for atmospheric waves in the upper atmosphere and the first direct measurements of isotopes of nitrogen, carbon, and argon, which reveal interesting clues about the evolution of the atmosphere. The bulk composition and thermal structure of the moon's upper atmosphere do not appear to have changed considerably since the Voyager 1 flyby.

This Report documents neutral composition measurements made with the INMS during the first low-altitude pass through Titan's upper atmosphere by the Cassini-Huygens spacecraft on 26 October 2004. During the ±15 min before and after its closest approach, INMS acquired a rich data set of information on Titan's atmospheric composition and structure covering an altitude range from 3000 to 1174 km. The closest approach occurred at 38.774° latitude, 88.45° west longitude at a solar local time of 16.753 hours. The highest priority objective of the Cassini orbiter during the first flyby was to measure the densities of the major atmospheric constituents N_2 and CH_4 and the inferred thermal structure between 1174 and 2000 km, because these data were important in planning the Huygens probe insertion and subsequent Cassini orbiter flybys. However, these measurements and subsequent analysis yielded substantial scientific results, including (i) the existence of large-amplitude (~10 K) and large–spatial scale (~180 km) atmospheric waves between 1100 and 1500 km, (ii) the identification of a suite of carbon-nitrile compounds at higher altitudes than anticipated (~1200 km), and (iii) the determination of the isotopic ratios of nitrogen in N_2, carbon in CH_4, and the abundance of ^{40}Ar as well as an upper limit for the mixing ratio of ^{36}Ar. We begin with a brief description of the instrument, then present the data set, and finish with a discussion of the major results enumerated above.

INMS is a dual–ion source quadrapole mass spectrometer covering the mass range of 0.5 to 8.5 and 11.5 to 99.5 daltons (*1*, *2*). The dual-source design combines classic closed and open ionization source configurations designed to measure inert species and reactive species and ions, respectively. The primary data reported in this paper were obtained with the closed source, which is designed to measure nonreactive atmospheric gases. In the closed source, the neutral gas flows into a spherical antechamber where it thermally accommodates with the walls of the antechamber before flowing through a transfer tube to an electron ionization source; there, the gas is ionized by an electron impact at 70 eV. The high flyby velocity of the Cassini spacecraft with respect to Titan (~6 km s^{-1}) produces a dynamic pressure enhancement in the antechamber, which increases sensitivity (*1*, *2*). Reactive species are not measured in this configuration.

Ionization of the primary constituents N_2 and CH_4 by the electron ionization source produced not only the primary ions N_2^+ and CH_4^+ but also dissociative fragments (over-

[1]Department of Atmospheric, Oceanic, and Space Sciences, University of Michigan, Ann Arbor, MI 48109–2143, USA. [2]NASA Goddard Space Flight Center, Greenbelt, MD 20771, USA. [3]Lunar and Planetary Laboratory, University of Arizona, 1629 East University Boulevard, Tucson, AZ 85721–0092, USA. [4]Department of Physics and Astronomy, University of Kansas, Lawrence, KS 66045, USA. [5]Space Sciences Laboratory, University of California, Berkeley, CA 94720, USA. [6]Applied Physics Laboratory, Johns Hopkins University, Laurel, MD 20723, USA. [7]Institute of Astronomy, National Central University, Chung-Li 32054, Taiwan. [8]Space and Atmospheric Physics Group, Imperial College, London SW7 2BW, UK. [9]Southwest Research Institute, Post Office Drawer 28510, San Antonio, TX 78228–0510, USA.

bars in Fig. 1). It also measured a host of ions and fragments due to minor atmospheric species (H_2, C_2H_2, C_2H_4, C_2H_6, C_3H_4, and Ar).

All of the measurable product channels were determined during the flight unit and engineering unit calibrations (with the exception of C_2N_2, C_3H_4, C_4H_2, HCN, and HC_3N, which were obtained from National Institute of Standards and Technology tabulations) and are subsequently used in the deconvolution of the spectra. The spectrum displayed in Fig. 1 (acquired every 4.6 s between the altitudes of 1230 and 1174 km and which can be co-added to enhance the signal-to-noise ratio) includes a mass scan covering the range from 1 to 99 daltons. This altitude range was chosen to be within approximately one atmospheric scale height of the Cassini closest approach (CA) altitude. The signal in each mass bin is a combination of the signals from the ionization or dissociative ionization of several species. Calibration data provide the sensitivity and the distribution of the dissociation products. Spacecraft velocity and altitude are used to compute the ram flow enhancement. From this data, a matrix is constructed relating instrumental response for various mass channels to the atmospheric composition. An inversion of this matrix with suitable numerical methods (*3*) yields abundances for a range of species. The measurements (and matrix elements) are weighted by the reciprocal measurement error.

Using two independent methods, we found the derived volume-mixing ratio of methane to be between 2.2 and 2.7% (for the first and second method, respectively) in the upper atmosphere. For the first method, we calculated the average ratio from the mass deconvolution of the average spectra between 1230 and 1180 km in the ingress data set as described above; for the second method, we used a diffusion model containing CH_4 and H_2 with an altitude-independent eddy diffusion coefficient and temperature as free parameters to fit the data in the altitude range of 1174 to 1500 km. The temperature structure between 1174 and 1500 km was found to be isothermal with a temperature (±SD) of 149 ± 3 K for the combined ingress and egress N_2 and CH_4 data sets (Fig. 2). A weak horizontal temperature gradient (~2 K/1000 km) was seen between ingress (145.8 K) and egress (151.8 K). From Fig. 2 we also note the close agreement of the present observations with the Voyager ultraviolet spectrometer data [reanalysis by Vervack (*4*)]. The extension of the INMS density profile (solid line) to lower altitudes in this case is with the assumption of a 149 K isothermal profile down to 900 km.

Some other important atmospheric quantities can also be derived from the density measurements. An eddy coefficient of $K = 4.2 \times 10^9$ cm^2 s^{-1} was determined by fitting the combined set of ingress and egress data ($K = 1.6 \times 10^9$ cm^2 s^{-1} was found for ingress data alone and $K = 8.3 \times 10^9$ cm^2 s^{-1} for egress data). Adequate fits were obtained assuming constant K with altitude. These values imply a homopause altitude defining the boundary between the well-mixed and diffusively separated portions of the atmosphere; the altitude was calculated by finding the intersection between K and the N_2-CH_4 binary diffusion coefficient profiles. We found the homopause at 1195 ± 65 km. Finally, the exobase above which the mean free path of a particle is equal to the atmospheric scale height was calculated from the measured densities to be at an altitude of 1429 ± 5 km.

We observed strong temperature perturbations superimposed on the isothermal profile derived from altitude analysis of the combined ingress and egress N_2 and CH_4 data sets. These perturbations along the spacecraft track can be mapped either horizontally or vertically and appear to represent either a vertically propagating oscillation or an intrinsic harmonic of the atmosphere. Only the vertical mapping case is presented in Fig. 3, suggesting a wave amplitude of 10 K and a vertical wavelength of 180 km. The origin of these waves in Titan's upper atmosphere could be an energy or momentum source located at lower altitudes in the

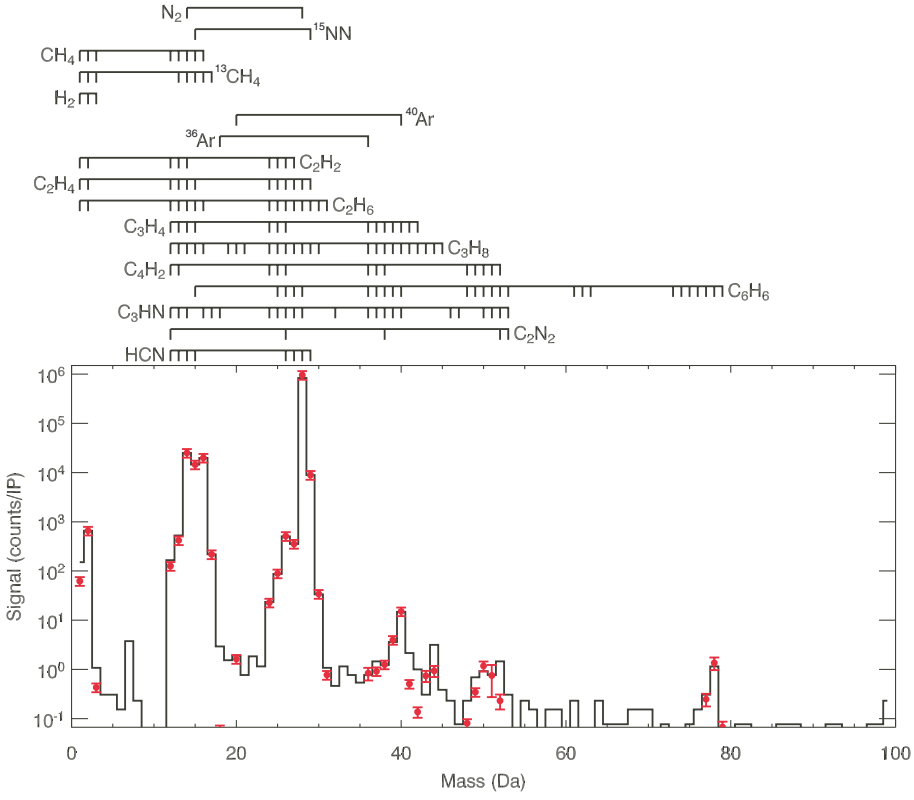

Fig. 1. The average mass spectrum from 1 to 99 daltons measured by INMS on the 26 October flyby (T_A) between the altitudes of 1174 and 1230 km. The average spectrum includes only inbound data where the INMS was pointed along the spacecraft velocity vector. The solid black line represents the measured, background-corrected spectra and the red circles represent the reconstructed spectra using the values of Table 1. The error bars displayed are the larger of the 20% calibration uncertainty or the 1σ statistical uncertainty. counts/IP, counts per integration period. The bars above the graph indicate the mass/charge locations of the ionization and dissociative ionization fragments of the species indicated.

Table 1. Minor species determined from the mass spectral deconvolution with 1σ error. C_6H_6 may represent a contaminant. Data are expressed in values of the mole fraction. C_2H_4 value depends on the value adopted for HCN. The following species were identified at less than 5 ppm: C_3H_8, C_4H_2, HCN, HC_3N, C_6H_6, and C_2N_2.

Species	INMS-derived values	CIRS values (*7*)
CH_4	$2.19 \times 10^{-2} \pm 0.002 \times 10^{-2}$	$1.6 \times 10^{-2} \pm 0.5 \times 10^{-2}$
H_2	$4.05 \times 10^{-3} \pm 0.03 \times 10^{-3}$	Not measured
C_2H_2	$1.89 \times 10^{-4} \pm 0.05 \times 10^{-4}$	$3.3 \times 10^{-6} \pm 0.3 \times 10^{-6}$
C_2H_4	$2.59 \times 10^{-4} \pm 0.70 \times 10^{-4}$ to $5.26 \times 10^{-4} \pm 0.08 \times 10^{-4}$	$1.6 \times 10^{-7} \pm 0.7 \times 10^{-7}$
C_2H_6	$1.21 \times 10^{-4} \pm 0.06 \times 10^{-4}$	$2.3 \times 10^{-5} \pm 0.4 \times 10^{-5}$
C_3H_4	$3.86 \times 10^{-6} \pm 0.22 \times 10^{-6}$	$1.2 \times 10^{-8} \pm 0.3 \times 10^{-8}$

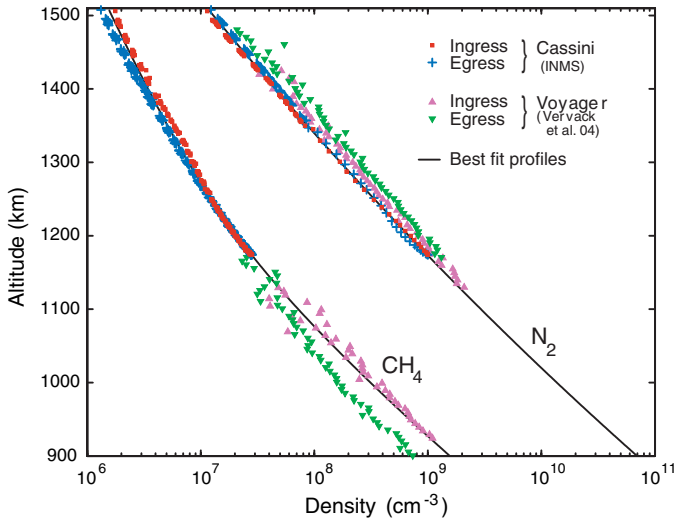

Fig. 2. The INMS-derived densities of methane (mass channel 16) and molecular nitrogen (mass channels 14 and 28) in red (ingress) and blue (egress) from T_A, compared with the Vervack-derived (*4*) values from Voyager ultraviolet spectrometer in pink (ingress) and green (egress). The solid black lines represent the best-fit densities, which correspond to a 149 K isothermal temperature profile. The methane mixing ratio from this modeling fit to the data is 2.7% at 1174 km.

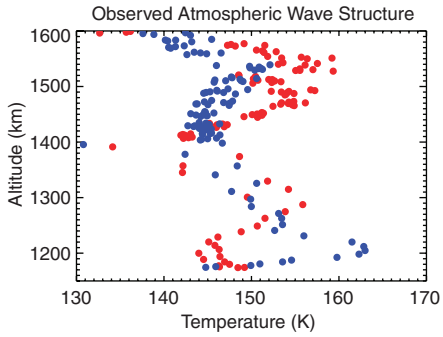

Fig. 3. Vertical profiles of temperature derived from observations of N_2 and CH_4 by INMS during T_A. Red data refer to ingress results and blue to egress.

atmosphere, or they could represent an external source from Saturn's magnetosphere, or both.

Analysis of an average spectra for the altitude range of 1230 to 1174 km near CA allowed us to determine a preliminary list of carbon-nitrile compounds and their abundances. The spectral fit from our deconvolution, discussed above, is shown in Fig. 1, and the resulting list of compounds is provided in Table 1. At this preliminary stage in the analysis, the abundances of molecular species are not well-established because we have not completed a thorough analysis of systematic uncertainties, most notably the interaction of potentially reactive species (such as HCN) with the wall of the antechamber for an impact velocity of ~6 km s^{-1}. However, we are confident in the detection of all species listed in the table.

The spectral analysis procedure also leads to a determination of isotopic ratios for nitrogen ($^{14}N/^{15}N$) and carbon ($^{12}C/^{13}C$), a determination of the ^{40}Ar mixing ratio, and an upper limit on the ^{36}Ar mixing ratio in the upper atmosphere. Because the lowest altitudes sampled by INMS on this first Titan flyby were evidently below the homopause, these volume-mixing ratio values can be used to infer mixing ratios for the well-mixed atmosphere at lower altitudes. The statistical error associated with determining the volume-mixing ratios by this method is on the order of 1%, but the uncertainties associated with the calibration data lead to an overall uncertainty of 20% (Table 2). However, the calibration uncertainties cancel for the isotopic ratios reported so that the only error sources are statistical or systematic errors introduced by the analysis method. Another method was also used to determine the isotopic abundances in which integrated sums of measured abundances (and errors) below 1230 km are used. The results of the two approaches are given in Table 2. There is good agreement between the methods for the carbon ratio, leading us to conclude that systematic errors are small and that statistical errors define the uncertainty. In the case of the nitrogen ratio, the saturation in the mass-28 channel required scaling of the low-sensitivity counter to replace data from the saturated high-sensitivity counter. At this time, the scale factor is not well-determined, resulting in systematic errors that are differential between the two methods. Thus we quote a range of values that define our uncertainty in this regard and we have verified the reported isotopic ratio value at higher altitudes where the N_2 data in channel 28 are not yet saturated.

INMS measurements obtained during the first pass of the Cassini orbiter through Titan's upper atmosphere lead to some important conclusions. A key finding is the apparent stability of the atmosphere over the 25 years since the Voyager flyby, as indicated by the comparison shown in Fig. 2. We suggest that this may be due to the thermostatic control exercised on the upper atmosphere by the infrared active species HCN. Another key result is the location of the homopause at ~1195 km, which is much higher than was expected [table 1 in (*1*)] (*5*). This result indicates that turbulent mixing extends to very high altitudes, and is consistent with the discovery by INMS of large scale–size and large-amplitude atmospheric waves in the upper atmosphere (Fig. 3). The large-scale size of the atmospheric waves was anticipated and is a consequence of atmospheric filtering by wind shears and thermal gradients at lower altitudes, and the large wave amplitude is within the limits of model predictions (*6*).

The existence of heavy hydrocarbon species at altitudes above 1200 km is another possible consequence of the well-mixed atmosphere. An alternative explanation is that previous determinations of the production rates for these chemical species at high altitudes are too small. Most of the observed compounds were identified earlier in the lower atmosphere [table 1 in (*1*)] (*5*). A comparison of INMS-derived high-altitude values with those determined in the lower atmosphere from Cassini Composite Infrared Spectrometer (CIRS) measurements (*7*) is shown in Table 1. Modeling and further analysis of the new atmospheric data will lead to explanations of the large abundance of complex hydrocarbons and nitriles at high altitudes.

The measured isotopic ratios have important implications for the evolution of the Titan atmosphere and interior over geological time. The isotopic ratios for nitrogen ($^{14}N/^{15}N$) and carbon ($^{12}C/^{13}C$) can be used to constrain the role of atmospheric escape and other physical and chemical processes in the Titan system. The $^{14}N/^{15}N$ ratio of 172 to 215 (Table 2) is between that of Mars and Earth, indicating either substantial escape of the atmospheric reservoir of nitrogen since capture or release from the interior or an initial source of nitrogen with an isotopic ratio closer to the solar wind value of 200 ± 55 (*8*, *9*). Comparison of these results with model results of Lunine *et al.* (*10*) is informative. If one assumes that the initial nitrogen isotopic ratios were similar to those of Earth [$^{14}N/^{15}N = 272.0 \pm 0.3$ (*11*)], that the exospheric temperature has remained near 150 K, and that the relative position of the homopause and exobase has remained unchanged over the course of atmospheric evolution, then the formulation of Lunine *et al.* combined with INMS measurements suggests a loss of atmospheric nitrogen over the history of the atmosphere by a factor of 1.7 ± 0.05 to 10 ± 5 from its original levels, depending on the efficiency (0 to 0.6) for dissociative fractionation of the isotopes. This also assumes that the upper end of the INMS measurement range for this ratio (i.e., 215) is representative of the present-day isotopic ratio. Correspondingly, if we use the lower end of the INMS-measured range (172), the range of atmospheric loss factor becomes 2.8 ± 0.2 to 100 ± 75. Clearly, it is hard to constrain the amount of atmospheric loss over geological time with the present data set. The quoted uncertainty is largely due to our imprecise knowledge of the position of the homopause and exobase. However, large uncertainties about the initial Titan isotopic ratio (*8*, *9*) and the role of dis-

Table 2. Key isotopic ratios measured by INMS (uncertainties are quoted as a 95% confidence interval).

Isotopic ratio	Integration method	Deconvolution method	Combined results	Estimated value at surface
$^{14}N/^{15}N$	$188\ ^{+14}_{-16}$	214 ± 1	$172 < {}^{14}N/^{15}N < 215$	$168 < {}^{14}N/^{15}N < 211$
$^{12}C/^{13}C$	95.6 ± 0.1	93.8 ± 1.9	95.6 ± 0.1	81
^{36}Ar mixing ratio	$<4 \times 10^{-7} \pm 1 \times 10^{-7}$	$<6 \times 10^{-7}$	$<5 \times 10^{-7} \pm 2 \times 10^{-7}$	Not applicable
^{40}Ar mixing ratio	$7.1 \times 10^{-6} \pm 0.1 \times 10^{-6}$	$7.3 \times 10^{-6} \pm 2.1 \times 10^{-6}$	$7.1 \times 10^{-6} \pm 0.1 \times 10^{-6}$	

sociative fractionation limit us to conclude only that the Titan atmosphere was at least 50% denser in the past.

A perplexing aspect of the nitrogen isotopic ratios comes from comparing the INMS-measured molecular nitrogen isotopic ratio value to earlier ground-based determinations of $^{14}N/^{15}N$ in HCN measured in Titan's stratosphere (*12*, *13*). The HCN-derived values show enrichment of the heavier isotope of nitrogen that is more than a factor of 2 larger than the INMS-measured values for the molecular nitrogen isotope ratio. Chemical fractionation is the most likely source of the difference, but estimates so far do not come close to explaining the difference (*14*, *15*).

The heavy isotope enrichment of nitrogen stands in contrast to the carbon isotopic ratio ($^{12}C/^{13}C = 95 \pm 1$). The ratio is well-determined and slightly above the terrestrial value of 89.01 ± 0.38, but certainly within the present constraints of determinations for Jupiter (94 ± 12) and Saturn (89^{+25}_{-18}) (*10*). This suggests that the methane in the atmosphere is being replenished by an interior source at a rate fast enough that escape is not the dominant effect on the isotopic ratio. This is consistent with our understanding of photodissociation rates for methane and the associated deposition of complex hydrocarbons on the surface. This dissociation process acts as the dominant sink for the atmospheric portion of the carbon cycle on Titan. INMS measurements of H_2 outflow can help quantify this process. H_2 is a byproduct of the methane photodissociation, and the measured H_2 escape rate of $6.1 \times 10^9 \pm 0.2 \times 10^9$ cm^{-2} s^{-1} represents a photodissociation rate of 5×10^{27} methane molecules per second and an atmospheric carbon residence time of 5×10^7 years. However, this does not explain the elevated isotopic ratio value indicating an increase of the light ^{12}C isotope relative to the ^{13}C isotope when compared with the terrestrial value of 89.01 ± 0.38 (*11*). Such a light isotope enhancement on Earth of up to ~10% is associated with biology (*16*); on Titan a more likely process involves vapor pressure isotope effects at the surface (*17*). However, using a diffusion model and our present estimate of thermal structure and atmospheric diffusion to propagate the upper atmospheric value to the surface (Table 2), we obtained a surface value of 81, which is below the terrestrial value. Clearly, combining the INMS data with information obtained by the Huygens Gas Chromatograph Mass Spectrometer is necessary to reach closure on this issue.

The volume-mixing ratios of the isotopes of argon can be used to study both interior and accretion processes. ^{40}Ar is likely produced by radioactive decay of ^{40}K, as it is on Earth, and therefore the mixing ratio of ^{40}Ar can be compared to estimates of the radiogenic production and release of potassium in the mantle rocks. The measured ^{40}Ar is $7.081 \times 10^{-6} \pm 0.1 \times 10^{-6}$ as compared with an upper limit of 0.05 to 0.07% set by McKinnon's estimate (*18*). This suggests either that the outgassing of the interior has an efficiency of ~1% or (less likely) that the ^{40}Ar was lost to space at an early phase of atmospheric evolution. On the other hand, the nondetection of ^{36}Ar and ^{38}Ar may suggest that N_2 was not trapped in nebula ices in the form of clathrate hydrates (*19*–*22*). The upper limit of less than 6×10^{-7} by volume set by INMS for the ^{36}Ar abundance ratio leads to the conclusion that the nitrogen in the moon's atmosphere was not brought to Titan as N_2 trapped in clathrates but was likely derived initially from ammonia ice or ammonia hydrate formed in the local Saturn nebulae (*23*) or in the solar nebula (*24*) and subsequently converted to N_2 by photochemical processes (*25*) and/or from high-temperature shock formation of N_2 (*26*).

The first measurements of Titan's neutral composition in the upper atmosphere lead to a number of notable conclusions about the current atmospheric structure and about the evolution of Titan's atmosphere and interior. The atmosphere likely formed from the outgassing after planetesimals composed of silicates, water ice, clathrates of methane, and ammonia hydrates coalesced to form the moon. Subsequent photochemistry and/or shock-induced chemistry likely converted the atmospheric nitrogen into molecular nitrogen. The early atmosphere was 1.6 to 100 times more substantial and was lost through escape over the intervening 4.5 billion years due to the reduced gravity associated with the relatively small mass of Titan. Carbon in the form of methane has likely continued to outgas over time from the interior, given that much of its subsequent photolysis products have been deposited in the form of complex hydrocarbons on the surface (~5×10^{27} s^{-1} as estimated from the H_2 escape rate of $6.1 \times 10^9 \pm 0.2 \times 10^9$ cm^{-2} s^{-1} measured by INMS) and some of it has also been lost to space [2×10^{25} s^{-1} as estimated from modeling of the exospheric loss of carbon (*27*)]. The carbon isotopes in the upper atmosphere appear to be isotopically light due to atmospheric diffusion effects or vapor phase isotope effects at the surface resulting from condensation, evaporation, and sublimation of surface methane.

References and Notes

1. J. H. Waite *et al.*, *Space Sci. Rev.* **114**, 113 (2005).
2. W. K. Kasprzak *et al.*, *Proc. SPIE* **2803**, 129 (1996).
3. W. H. Press, B. P. Flannery, S. A. Teukolsky, W. T. Vetterling, *Numerical Recipes* (Cambridge Univ. Press, Cambridge, 1986).
4. J. R. Vervack, B. R. Sandel, D. F. Strobel, *Icarus* **170**, 91 (2004).
5. A. Coustenis *et al.*, *Icarus* **80**, 54 (1989).
6. D. F. Strobel, B. Sicardy, in *Huygens Science Payload and Mission* (ESA Special Publication SP-1177, Noordwijk, Netherlands, 1997), pp. 299–311.
7. Lower atmosphere values of the hydrocarbon mixing ratios at a pressure of 1.5 to 3.0 mbar and a latitude of 39° were taken from Flaser *et al.* (*28*). The methane value comes from the same reference but at a pressure of 3 to 20 mbar.
8. R. Kallenbach *et al.*, *Astrophys. J.* **507**, L185 (1998).
9. If instead of the solar wind value, we choose initial values close to the newly determined protonebula value (430), determined by Owen *et al.* (*29*), the requirement for escape is much larger than our assumption of a terrestrial initial value of 272.
10. J. I. Lunine *et al.*, *Planet. Space Sci.* **47**, 1291 (1999).
11. B. Fegley, in *Global Earth Physics: A Handbook of Physical Constants*, T. Ahrens, Ed. (American Geophysical Publications, Washington, DC, 1995), pp. 320–345.
12. M. A. Gurwell, *Astrophys. J.* **616**, L7 (2004).
13. T. Hidayat *et al.*, *Icarus* **126**, 170 (1997).
14. One likely mechanism for the enrichment of $HC^{15}N$ is the photoinduced isotopic fractionation effect (PHIFE) proposed by Yung and Miller (*30*). However, a preliminary estimate by Yung (*31*) shows that the magnitude of PHIFE for HCN is not sufficient to account for the observed enrichment.
15. Another possibility is ion-neutral reactions as studied in the case of the interstellar medium by R. Terzieva and E. Herbst (*32*), but such effects have not been examined at Titan temperatures (150 K).
16. M. J. Whiticar, *Chem. Geol.* **161**, 291 (1999).
17. Because methane is near the triple point near the Titan surface, one would expect a heavy isotope depletion of the gas as compared with the liquid or solid due to vapor pressure isotope effects similar to those observed for H_2O on Earth (*33*).
18. William B. McKinnon, personal communication. McKinnon assumes an anhydrous rock mass fraction for Titan of 0.55 ± 05 and a CI carbonaceous [K = 550 parts per million (ppm)] or H chondrite (780 ppm) composition for the rock (*34*). Of a primordial $^{40}K/K = 1.47 \times 10^{-3}$, 9.6% has decayed to ^{40}Ar. Perhaps we shouldn't be surprised by the very low degassing efficiency. If we assume that Titan has a rock core and that core was volcanically active, those magmas would still be erupting at great depths, and at pressures around 2 GPa. There is no thermodynamic incentive for volcanics to degas at such pressures.
19. T. Owen, *Planet. Space Sci.* **30**, 833 (1982).
20. J. I. Lunine, D. J. Stevenson, *Astrophys. J. Suppl. Ser.* **58**, 493 (1985).
21. T. Owen, *Planet. Space Sci.* **48**, 747 (2000).

22. F. Hersant *et al.*, *Space Sci. Rev.* **114**, 25 (2004).
23. J. I. Lunine, D. J. Stevenson, *Icarus* **70**, 61 (1987).
24. O. Mousis *et al.*, *Icarus* **156**, 167 (2002).
25. S. K. Atreya, T. M. Donahue, W. R. Kuhn, *Science* **201**, 611 (1978).
26. C. P. McKay *et al.*, *Nature* **332**, 520 (1988).
27. T. E. Cravens *et al.*, *Planet. Space Sci.* **45**, 889 (1998).
28. F. M. Flasar *et al.*, *Science* **308**, 975 (2005).
29. T. Owen, P. R. Mahaffy, H. B. Niemann, S. Atreya, M. Wong, *Astrophys. J.* **553**, L77 (2001).
30. Y. L. Yung, C. E. Miller, *Science* **278**, 1778 (1997).
31. Y. L. Yung, personal communication.
32. R. Terzieva, E. Herbst, *Mon. Nat. R. Astron. Soc.* **317**, 563 (2000).
33. T. F. Johns, in *Atomic Energy Research Establishment, Harwell: A Brief Guide* (GP/R-2166, Atomic Energy Research Establishment, Harwell, UK, 1957).
34. K. Lodders, B. Fegley, *The Planetary Scientist's Companion* (Oxford Univ. Press, New York, 1999).
35. We thank the Cassini project at NASA/Jet Propulsion Laboratory for financial support through contract #1228303; the flight and instrument teams for many years of dedicated effort; the Cassini Interdisciplinary Scientists T. Owens, D. Gautier, and J. Lunine for many helpful discussions; and several members of the Space Science community, K. Freeman, J. Kasting, R. Dissly, Y. Yung, and W. McKinnon for additional discussions.

3 February 2005; accepted 13 April 2005
10.1126/science.1110652

REPORT

Cassini Measurements of Cold Plasma in the Ionosphere of Titan

J.-E. Wahlund,[1]* R. Boström,[1] G. Gustafsson,[1] D. A. Gurnett,[2] W. S. Kurth,[2] A. Pedersen,[3] T. F. Averkamp,[2] G. B. Hospodarsky,[2] A. M. Persoon,[2] P. Canu,[4] F. M. Neubauer,[5] M. K. Dougherty,[6] A. I. Eriksson,[1] M. W. Morooka,[1] R. Gill,[1] M. André,[1] L. Eliasson,[7] I. Müller-Wodarg[6]

The Cassini Radio and Plasma Wave Science (RPWS) Langmuir probe (LP) sensor observed the cold plasma environment around Titan during the first two flybys. The data show that conditions in Saturn's magnetosphere affect the structure and dynamics deep in the ionosphere of Titan. The maximum measured ionospheric electron number density reached 3800 per cubic centimeter near closest approach, and a complex chemistry was indicated. The electron temperature profiles are consistent with electron heat conduction from the hotter Titan wake. The ionospheric escape flux was estimated to be 10^{25} ions per second.

The giant planet Saturn and its magnetosphere rotate with a period of ~11 hours, which can be inferred from radio measurements (*1*). At the distance of the large moon Titan [20 Saturn radii (R_S)], this corotation causes a magnetospheric plasma flow of several hundred kilometers per second that affects the upper ionized part of the thick atmosphere of Titan. Atoms and molecules in the upper atmosphere are ionized by solar ultraviolet (UV) radiation and by impacts of energetic particles that originate mainly from the magnetosphere. The aeronomic and electrodynamic processes involved in the interaction further produce a complex organic chemistry within the nitrogen- and methane-rich atmosphere of Titan as well as a loss of atmospheric constituents, providing in turn a source of plasma for the magnetosphere of Saturn (*2*).

The two first flybys of Titan (T_A and T_B) on 26 October and 13 December 2004 were very similar. Both occurred at 10.5 Saturn local time (LT) near the front side of Saturn's magnetosphere, and both approached inbound from the sunlit side and through the wake of Titan (Fig. 1). The outbound passes partly traversed a shaded region caused by Titan's thick atmosphere at a latitude of 30° to 40°N.

The structure and thermal state of the ionosphere of Titan were affected by the saturnian magnetosphere all the way down to closest approach (1176 km) during both flybys (Figs. 2 and 3). The general shape of the two main number density maxima near closest approach in Fig. 2 is broadly consistent with photoionization by UV light from the Sun and impact ionization by magnetospheric electrons (*3*, *4*). However, the plasma density was otherwise very structured and could be related to similar structures in the magnetic field data. The density data in Figs. 2 and 3 were collected at a high time resolution (20 samples/s) and are derived from the probe current at a constant bias voltage (~ +10 V), corrected for electron temperature and adjusted to fit the potential sweep data points for density. The LP sensor (*5*) samples the total electron number density surrounding the spacecraft, which includes the naturally occurring plasma electrons as well as a nearly constant level of photoelectrons around the spacecraft. The spacecraft-generated photoelectrons dominated the magnetospheric part of the flyby. According to measurements by the Cassini Plasma Spectrometer (CAPS), the magnetospheric electron density near Titan was just below 0.1 cm^{-3} during T_A (*6*).

The calculated magnetic pressure ($B^2/2\mu_0$) of the magnetosphere and the electron thermal pressure ($n_e k_B T_e$) of the ionosphere (where B is magnetic field strength, μ_0 is magnetic permeability, n_e is electron number density, k_B is the Boltzmann constant, and T_e is electron temperature) were largely of the same order of magnitude during the T_A flyby (Fig. 2B). Both flybys traversed the wake of Titan, and the effect of the magnetospheric dynamic pressure ($n_i m_i v_i^2/2$, where n_i is ion number density, m_i is average ion mass, and v_i is ion ram velocity) should therefore be small near closest approach. The ionopause, the region where the ionospheric thermal pressure balances the magnetospheric pressure, covered an extended region on both the inbound and outbound trajectories (yellow area in Fig. 2). The close relationship between cold plasma density signatures and magnetic field fluctuations and comparable values of ionospheric electron thermal and magnetospheric magnetic field pressures confirms the view that the saturnian magnetosphere is important for the structure and dynamics in Titan's ionosphere.

The Titan wake "neutral" sheet, where the magnetic field sharply rotates and relates to an electrical current, was identified by the Dual-Technique Magnetometer (MAG) near 15:35 UT (*7*). At this time, the RPWS LP detected a sharp peak in both electron number density (850 cm^{-3}) and electron thermal pressure (900 eV/cm^3). The altitude thickness of the compressed plasma sheet was 60 km, which is on the order of the ion gyroradius.

The LP provides estimates of n_e and T_e, but under some circumstances, values can also be obtained for m_i, v_i, n_i, ion temperature (T_i), solar UV intensity, and spacecraft potential. An estimate of the effective ion temperature ($T_{i,eff}$), which is the sum of the thermal random ion temperature and the ram ion directed flow energy [$T_{i,eff} = T_i + (m_i v_i^2/2e)$, expressed

[1]Swedish Institute of Space Physics, Box 537, SE-751 21 Uppsala, Sweden. [2]Department of Physics and Astronomy, University of Iowa, Iowa City, IA 52242, USA. [3]Department of Physics, University of Oslo, NO-0316 Oslo, Norway. [4]Centre d'Etude des Environnements Terrestre et Planétaires/CNRS/Institut Pierre Simon Laplace, 78140 Vélizy-Villacoublay, France. [5]Institute for Geophysics and Meteorology, Köln University, D-50923 Köln, Germany. [6]Blacket Laboratory, Imperial College London, London SW7 2BW, UK. [7]Swedish Institute of Space Physics, Box 812, SE-981 28 Kiruna, Sweden.

*To whom correspondence should be addressed. E-mail: jwe@irfu.se